ORIGINAL ARTICLE

Effect of TiAlSiN coating residual stress on its sliding wear and cutting wear performance

Zhenyu Wu[1,2] · Guangming Zheng[1,3] · Jiwang Yan[4] · Xiang Cheng[1] · Huanbao Liu[1] · Xianhai Yang[1]

Abstract

It is indispensable to explore the appropriate level of surface residual stress to enhance the wear resistance of coated tools. TiAlSiN-coated carbide tools with dissimilar surface residual compressive stresses ($-300 \sim -600$ MPa) are acquired via micro-sandblasting, which are used in the high-speed sliding friction experiments and turning experiments. The influence of residual stress on the sliding wear and cutting wear performance of TiAlSiN coated tools is investigated. The results show that with the improvement of surface residual compressive stress (absolute value), the friction coefficient and wear rate are reduced. The sliding wear resistance of the coated tool is enhanced. In addition, the cutting performance of the tool is also improved with the increase of residual compressive stress (absolute value). However, the excessive surface residual compressive stresses (absolute value) can lead to severe coating peeling, which in turn impairs the capability of wear resistance. The TiAlSiN-coated carbide tool with the stress of -500 MPa presents the best wear resistance in the high-speed sliding wear and cutting wear process.

Keywords Residual stress · Coated tools · Wear resistance · Sliding wear · TiAlSiN · Ti6Al4V

1 Introduction

Coated carbide tools are extensively used in machining and manufacturing because of great hardness, temperature resistance, and low friction coefficient [1, 2]. However, coated tools are prone to problems such as large fluctuations in cutting force and excessive cutting temperature when cutting titanium alloys, superalloys, and other difficult-to-machine materials in high-speed and dry condition, leading to increased tool wear and reduced tool life [3, 4].

The increase of energy consumption will inevitably cause more damage to the ecological environment, and the energy

consumption and environmental problems in the cutting process have become the focus of researchers [5, 6]. High-speed cutting and dry cutting are considered green machining processes that help reduce energy consumption and prevent environmental pollution [7]. For improving processing efficiency to reduce energy consumption and environmental pollution, it is important to enhance the wear resistance of coated tools, which has an enormous influence for the tool life.

Surface residual stress has a momentous effect on the cutting performance of the coated insert. Because of the stress and thermal alternating loads during the cutting process, residual compressive stress is beneficial to the coated insert [8, 9]. In the literature related, the residual stress of coated tools has an important effect on tool wear in turning of AISI4140 and Ti6Al4V [10]. Increasing the residual compressive stress of the PVD-TiAlN coating, the ability of coated tools to resist adhesive wear and chipping is improved accordingly. In addition, during milling of HSS HS6-5-3C with TiAlCrSiN-coated tools, the increase in compressive residual stress can prevent the propagation of cracks and enhance the cutting capability of coated tools. However, excessive residual compressive stress may lead to the separation of the TiAlCrSiN coating from the

✉ Guangming Zheng
zhengguangming@sdut.edu.cn

1 School of Mechanical Engineering, Shandong University of Technology, 266 West Xincun Road, Zibo 255000, China

2 Shinva Medical Instrument Co., Ltd, 7 Taimei Road, Zibo 255000, China

3 Shandong Key Laboratory of Precision Manufacturing and Special Processing, Zibo 255000, China

4 Department of Mechanical Engineering, Faculty of Science and Technology, Keio University, 3-14-1 Hiyoshi, Kohoku-Ku, Yokohama 223-8522, Japan

carbide substrate [11]. Either the residual compressive stress is too low or too high, it will lead to increased abrasive wear. Moreover, the wear of ZrCN and TiN-coated tools is directly related to the coating stresses. Excessively high stresses may lead to high tool flank wear, resulting in shortening of tool life [12].

In addition, the surface residual stress has crucial influence on the capability of sliding friction and wear of coated carbide tools. For PVD-TiAlN coatings, the increase in residual stress can promote the wear resistance of the tool [13]. The surface residual stress of the WC-CoCr-based high-velocity oxy fuel (HVOF) coatings increases after grinding, resulting in an increase in the microhardness of the coating, which further enhances the wear resistance [14]. There is also a literature finding that the sliding wear of HVOF Inconel 625 coating is related to the compressive residual stress [15]. However, one study indicates that high residual stress will reduce the adhesion strength of PVD-AlTiSiN + TiSiN coating tools, which leads to coating peeling, and the tool wear resistance will decrease [16]. Thus, an appropriate level of residual stress can significantly reduce tool wear. It is necessary to optimize the surface stress state of coated tools.

The residual stress of coated carbide tools is formed after a series of surface treatment processes, and each process step has an impact on the residual stress state [17]. Surface treatment of the substrate before coating deposition can change the residual stress of the coated tool. Grinding and polishing treatment processes produce residual compressive stress in the cemented carbide substrate but damage the thin coating layer [18]. Similarly, high residual compressive stress is induced after shot peening [19]. On the contrary, laser processing causes residual tensile stress on the surface of cemented carbide [20].

Physical vapor deposition (PVD) is a popular tool coating method. Because of the thermoelastic effect and grow-in defects of high kinetic energy particles during PVD, the coated layer usually has high residual stress, and the magnitude of residual stress depends on coating parameters, such as deposition speed, deposition temperature, and bias pressure [21]. Subsequent surface treatment will also change the magnitude of residual stresses.

Micro-sandblasting surface treatment technology is an effective method of improving coating performance by using abrasive particles to impact the coating [22–24]. For PVD-TiAlN coatings, after wet micro-sandblasting treatment, the hardness and fatigue life of the coating are improved with the increase of compressive stress. Particularly, the micro-sandblasting with Al_2O_3 abrasives leads to a significant increase in residual compressive stresses. The micro-sandblasting process parameters also affect the stress state of the coating. As the increase of blasting time and pressure, the surface residual stress of coated tools increases accordingly.

At present, the dissimilar levels of coating residual stress are acquired mainly with controlling the coating deposition parameters. There are few researches on the surface residual stress of TiAlSiN coated tools, and the appropriate residual stress level for TiAlSiN-coated tools needs to be revealed. This work aims at clarifying the cutting performance of PVD-TiAlSiN coated tools which have different surface residual stress states acquired through micro-sandblasting surface treatments, and revealing the appropriate surface residual stress level for PVD-TiAlSiN coated tools to obtain high wear resistance. The effects of surface residual stress on capability of wear resistance are elucidated via high-speed sliding friction turning of Ti6Al4V. This work will supply useful information for surface strengthening of coated tools and high-efficient machining using the coated tools.

2 Material and methods

2.1 Tool and workpiece material

The coated carbide cutting tool (Model CNMG120408-NM) was adopted, which was manufactured by Zhuzhou Diamond Cutting Tool Co., Ltd. The coating material was the TiAlSiN coating produced by physical vapor deposition (PVD) with a WC–Co cemented carbide substrate. The workpiece material was Ti6Al4V. The workpiece was a cylinder with a diameter of 100 mm and a length of 250 mm. Table 1 exhibits the main mechanical parameters of Ti6Al4V. Table 2 displays the elemental components of Ti6Al4V.

2.2 Micro-sandblasting experiment

The micro-sandblasting surface treatment of TiAlSiN coated tools was conducted. The surface integrity of the tool and micro-sandblasting parameters are shown in Table 3. Four kinds of coated tools S1, S2, S3, and S4 with different surface residual stress levels were obtained by micro-sandblasting. According to X-ray diffraction method, the surface residual stress of different coated tools was measured. The measuring instrument was an X-ray residual stress tester (Model X-stress 3000, Finland). During the measurement, the tube voltage and tube current were 20 kV and 2 mA, respectively. A collimating tube with a diameter of 2 mm was used. In addition, the X-ray wavelength was 0.2291 nm.
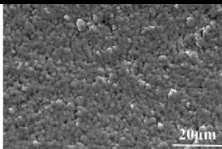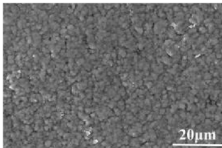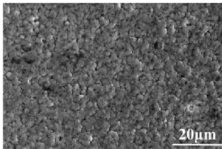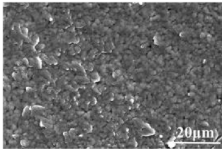
Table 1 Main mechanical parameters of Ti6Al4V

Hardness (HRC)	Impact toughness (J/cm²)	Yield strength (MPa)	Tensile strength (MPa)	Elastic modulus (GPa)
35 ± 5	400	834	932	114

Table 2 Elemental components of Ti6Al4V (wt%)

Al	V	Fe	C	N	H	O	Ti
5.5–6.8	3.5–4.5	0.30	0.10	0.01	0.015	0.2	Balance

Table 3 Surface integrity of the coated tools and micro-sandblasting parameters

| Tools	Surface integrity				Micro-sandblasting parameters	
	Residual Stress (MPa)	Surface Hardness (HV)	Surface roughness R_a (μm)	Surface morphology	Pressure p (Mpa)	Time t (s)
S1	-322±10	2230	0.205		0.2	5
S2	-414±16	2381	0.212		0.1	9
S3	-519±20	2440	0.209		0.3	3
S4	-631±18	2344	0.215		0.4	3

Moreover, the Ti element was used as the target material and the exposure time was 15 s. The surface residual stress of each coated tool was measured 5 times and averaged. For the four tools, the surface residual stress level was different. At the same time, the surface morphology and roughness of the tool can reduce the interference of other surface integrity on the wear resistance.

2.3 High-speed friction and wear experiment

Figure 1 presents the diagrammatic sketch of high-speed friction and wear experimental setup. The friction and wear experiment were conducted on the CDK6136i CNC lathe. The experiment tool and workpiece material were the same as the high-speed dry cutting experiment. The ring-block line contact friction method was used. The friction environment was dry condition, and the ambient temperature was room temperature. In order to avoid burning the coating at high temperature caused by high-speed rotating friction, the rotating speed of workpiece $n = 300$ r/min. During the experiments, the friction load was varied between 20 and 200 N. Preliminary experiments indicated that in the initial stage of direct contact between TiAlSiN coating and Ti6Al4V titanium alloy, the load changed greatly and was unstable. If the friction contact time was too long, the coating would be severely damaged and peeled off in a large area, leading to the exposure of substrate. Subsequent observation and analysis cannot be carried out normally. So, the sliding wear time was set to 30 s in the experiment. In the experiment, the fixed tool holder was used to apply the

Fig. 1 Diagrammatic sketch of high-speed friction and wear experimental setup
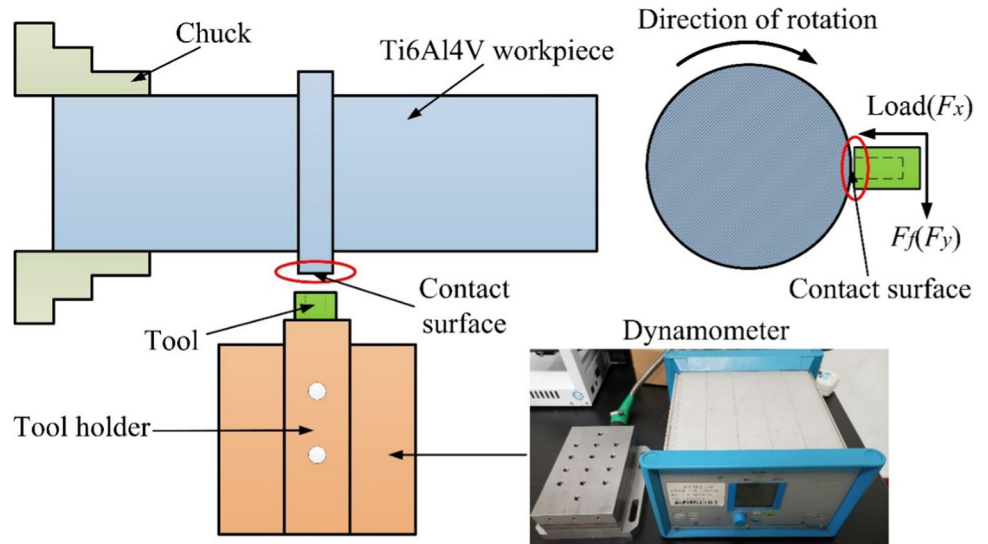
load F and the Kistler 9257B three-way dynamometer was applied to gauge and control the load F_x. The friction force was recorded using the dynamometer, and then, the friction coefficient was calculated.

The wear rate was calculated using the Coulomb friction and wear formula (1).

$$\mu = f/N \tag{1}$$

where μ represented the friction coefficient, f represented the sliding friction force F_y (N), and N represented the pressure load F_x (N). In order to reduce the error interference, each group of friction coefficient was gauged three times and averaged.

Comparison of wear rates was achieved by the tool wear volume. Figure 2 exhibits the schematic diagram of the definition of tool wear volume. The formula for computing the tool wear volume is shown in formula (2).

$$V = l[Lr/2 - (r-d)w/2] \tag{2}$$

where V represented the wear volume (mm^3), l represented the length of worn area (mm), L represented the arc length of section of worn area, r represented the radius of the workpiece

(mm), d represented the depth of worn area (mm), and w represented the width of worn area (mm). Each parameter was gauged three times and averaged.

In actual experiments, l was much larger than d, which was like L. Therefore, the value of L could be approximately regarded as l. So, formula (2) can be simplified to formula (3).

$$V = wld/2 \tag{3}$$

After the friction and wear experiment, the coated tool was cleaned with ultrasonic alcohol solution for 30 min. The morphology of the wear surface was obtained by the QUNTA250 scanning electron microscope, by which the average length and width of the worn area was also measured. The average depth of worn area was gauged by the UP-WLI white light surface profiler. According to formula (Eq. 3), the tool wear volume was calculated.

2.4 High-speed cutting experiment

The high-speed dry cutting experiment was implemented on a CDK6136i CNC lathe. Table 4 presents the cutting

Fig. 2 Schematic diagram of the definition of tool wear volume
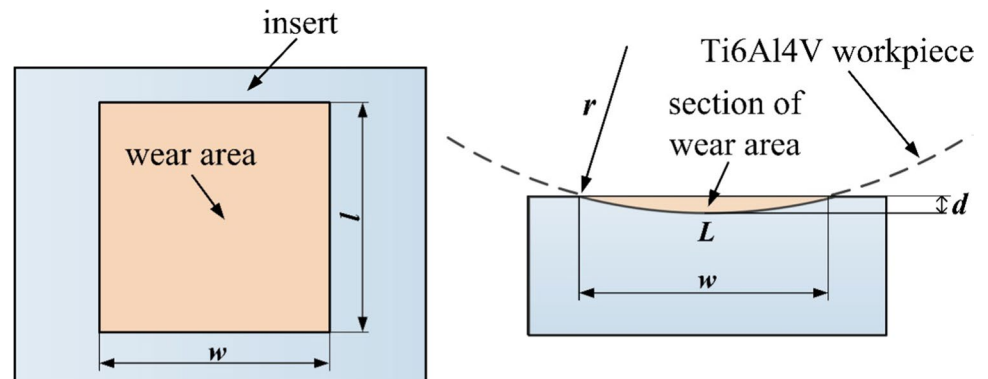
geometry parameters of TiAlSiN-coated tools. The model of the tool holder was TCLNR2020K12. The photographs of the high-speed turning setup are displayed in Fig. 3. The cutting method was continuous dry turning. The cutting speed $v = 120$ m/min, the feed rate $f = 0.2$ mm/r, and the cutting depth $a_p = 0.3$ mm.

A USB200 portable digital microscope was used to observe flank wear in the turning experiment. The average value of five measurement was selected. When the flank tool wear VB = 0.3 mm, the tool was considered as failure. The cutting force was gauged by the three-way dynamometer Kistler 9257B. The cutting temperature was gauged by the FLIR A615 infrared thermal imager, of which the measuring range was $-50 \sim 1200$ °C. After cutting experiments, the wear morphology of the coated tools was obtained by the QUNTA250 scanning electron microscope (SEM). Chips in the rapid wear stage of the coated inserts were collected, and the chip morphology was also observed.

Table 4 Geometry parameters of the coated tool

Nose radius r_ε (mm)	Cutting edge angle κ_r (°)	Inclination angle λ_s (°)	Rake angle γ_o (°)	Clearance angle α_o (°)
0.8	95	-5.5	6	7

# 3 Results and discussion

3.1 Sliding wear performance

3.1.1 Friction coefficient

The variation of the friction coefficient with sliding time is illustrated in Fig. 4. The friction coefficient of S1 with small compressive stress is larger among four coated tools. For S1, the fluctuation of friction coefficient is obvious. The smaller surface residual compressive stress leads to smaller hardness, which causes large friction coefficient of S1. The fluctuation phenomenon of S2 is significantly reduced, compared with S1. The
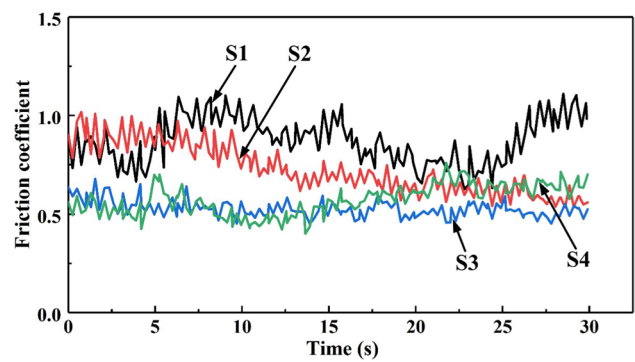
Fig. 4 Variation of the friction coefficient with sliding time

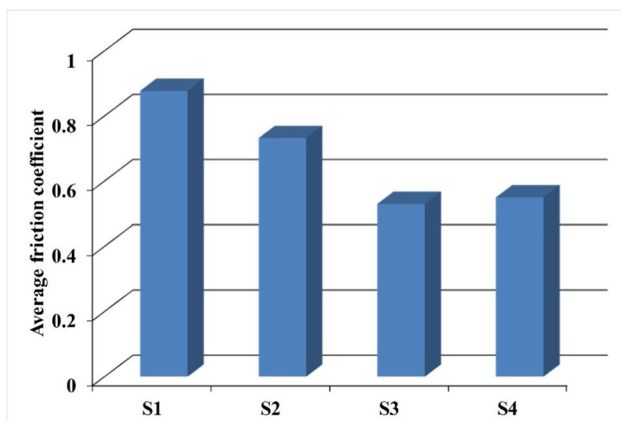**Fig. 3** Photographs of the high-speed turning setup
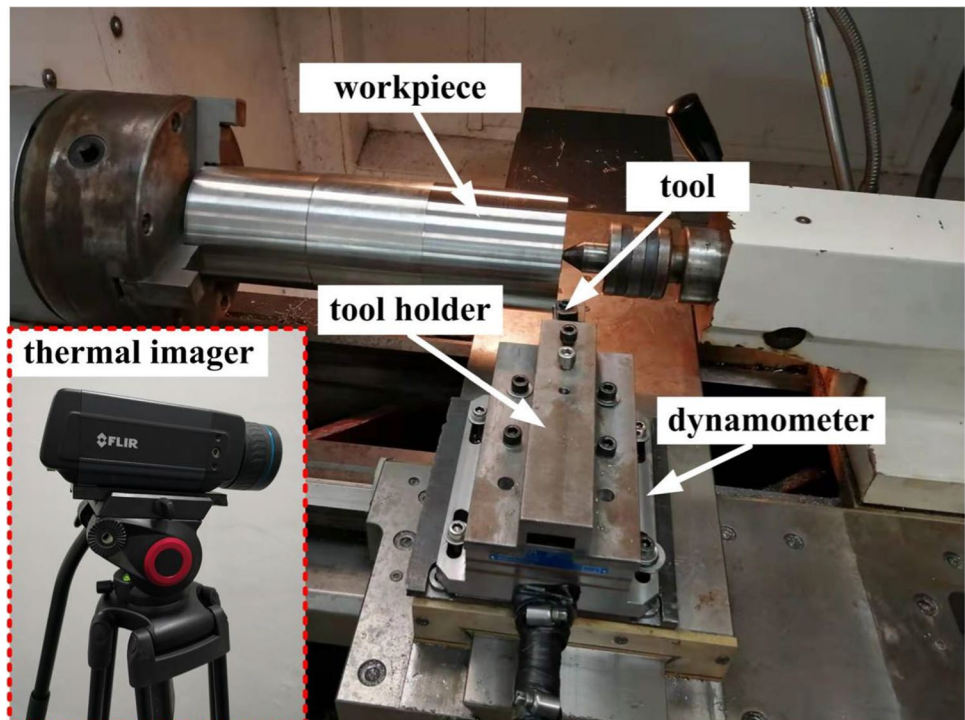
high surface compressive stress conduces to the intensification of wear resistance. So, the friction coefficient of S2 is less than that of S1.

During the initial and middle of sliding friction process, the friction coefficient of S3 is also significantly decreased. For S4 with compressive stress of − 600 MPa, the friction coefficient remains small in the initial sliding wear stage. With time increases, however, the size and fluctuation extent of the friction coefficient is gradually promoted. For tool S4, the relatively larger micro-sandblasting parameters inevitably reduces the coating thickness which affect the micro-hardness of coated tools. In addition, a larger coating compressive stress can result in the coating to separate from the substrate, making the tool friction coefficient and fluctuation range larger.
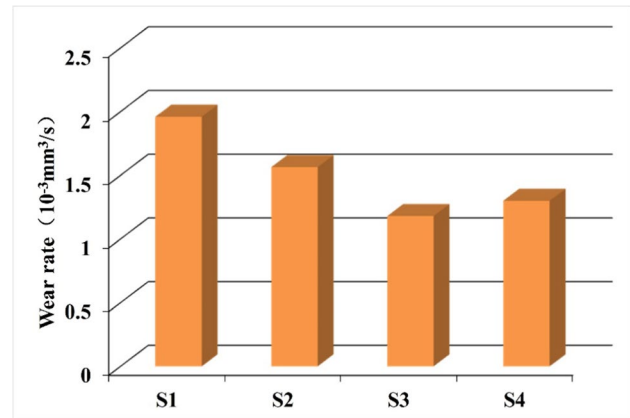
The average friction coefficient of the TiAlSiN coating with dissimilar surface residual stresses is expressed in Fig. 5. In general, the friction coefficient declines with the improvement of the surface compressive stress. Although the average friction coefficient of S3 and S4 tools are close, the friction coefficient and fluctuation extent of S4 is enhanced in the late of sliding friction process. Moreover, the sliding friction process is not stable. Therefore, the S3 tool with the residual compressive stress level of − 500 MPa has the best capability of resisting sliding wear.

3.1.2 Wear rate

The friction and wear rate of the TiAlSiN coating with dissimilar surface residual stresses is displayed in Fig. 6. The wear rate reflects the wear resistance of the tool. Under the same conditions, the smaller the wear rate of the tool means the smaller the amount of tool wear. Accompanied by the improvement of surface residual compressive stress, the wear rate decreases first and then increases (Fig. 6). The increase in surface residual compressive stress leads


Fig. 6 Wear rate of the TiAlSiN coating with dissimilar surface residual stresses

to high microhardness, which enhance the wear resistance of the tool. Thereby, the tool wear rate is reduced. The coated tool S3 with the surface residual compressive stress level of − 500 MPa has the lowest wear rate. This is consistent with the alter trend of the average friction coefficient (Fig. 5). From the wear rate of S4, however, excessive surface residual compressive stress can affect the bonding strength between the substrate material and the coating, causing the coating to peel off and take away the substrate material, thereby increasing the amount of tool wear. So, the wear rate of S4 increases instead. In summary, the increase of residual stress within a certain range is advantageous to ameliorate the wear resistance of coated tools.

3.1.3 Sliding wear mechanism

The SEM micrographs of the sliding wear on TiAlSiN coating with dissimilar surface residual stresses is exhibited in Fig. 7. During the friction wear process, a large amount of flake adhesion is distributed along the direction of the relative movement of the tool and the workpiece. The boundary of the wear area is obvious. Figure 8 exhibits the EDS of worn area A in Fig. 7a, where the presence of the coating material element V indicates that the Ti6Al4V material is bonded to the wear surface. The Ti6Al4V material has inferior capacity of heat-transmission. So, the workpiece and tool surface generate a lot of frictional heat on the contact surface. Moreover, the frictional heat is not easy to disperse. Thus, the high temperature promotes the mutual diffusion of active Ti elements and elements in coating, due to the high chemical activity of titanium alloy. Then, the adhesion points and aggravate wear is easy to form. Simultaneously, the elevated temperature will also soften the workpiece to produce plastic deformation, resulting in more titanium

Fig. 5 Average friction coefficient of the TiAlSiN coating with dissimilar surface residual stresses

Fig. 7 SEM micrographs of the sliding wear on TiAlSiN coating with dissimilar surface residual stresses, **a** S1, **b** S2, **c** S3, and **d** S4
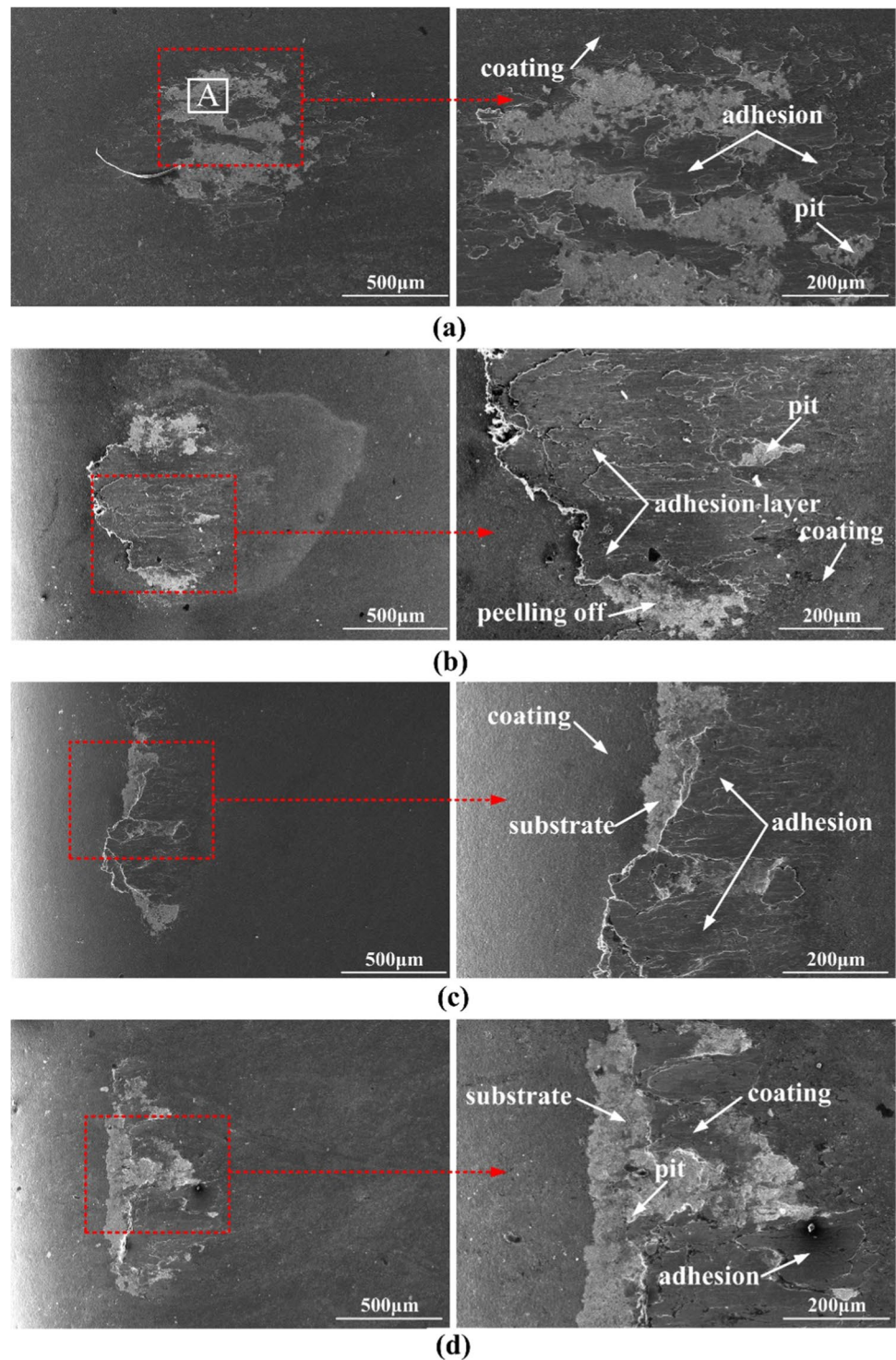
alloy material bonded to the tool surface under the impact of unstable friction load.

Under the impact of friction load, the adhesion layer on the contact surface of Ti6Al4V and TiAlSiN coating is easily peeled off. The spalling of the adhesion layer will concurrently remove part of the TiAlSiN material. So, the surface of all four coated tools shows coating peeling and a small number of pits (Fig. 7). The decrease of coating thickness reduces the thermal conductivity of the coated tool, resulting in a higher temperature in the peeling area of the coating. It is more likely to produce new adhesion and then fall off again. This repeated cycle will cause a large area of coating to peel off. When the adhesion peels off, the adhesive layer and coating material sheds off in the form of particles. These
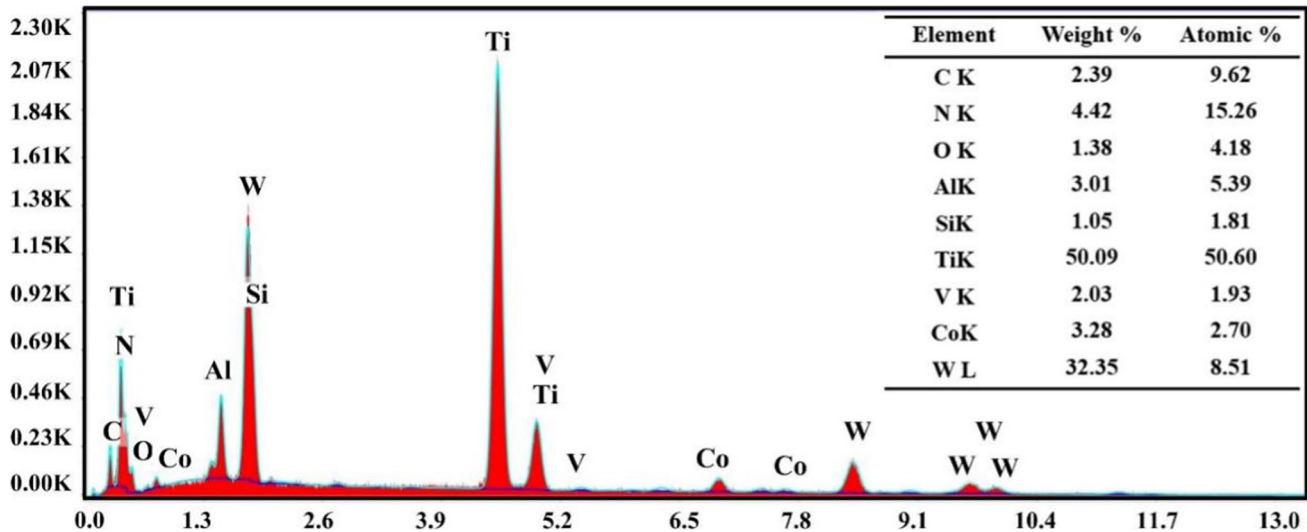
Element	Weight %	Atomic %
C K	2.39	9.62
N K	4.42	15.26
O K	1.38	4.18
Al K	3.01	5.39
Si K	1.05	1.81
Ti K	50.09	50.60
V K	2.03	1.93
Co K	3.28	2.70
W L	32.35	8.51

Fig. 8 EDS of worn area A in Fig. 7a

hard particles can scratch the coating surface, resulting in scratches and abrasive wear.

During the normal wear stage, a numerous cumulation of friction heat leads to a rapid increase in temperature. And the workpiece begins to bond on the coating surface, due to thermal softening and plastic flow. As the adhesion increases and the coating peels off, the influence of surface roughness on tool wear resistance gradually is reduced. Meanwhile, the surface residual stresses gradually dominate.

The cemented carbide elements such as W, C, and Co appear in the area A (Fig. 8), which further proves that the S1 tool has a wide range of exposed cemented carbide. This indicates that the adhesion strength between the coating and the substrate is low at the surface residual stress of -300 MPa and the coating is prone to spalling along with adhesion. With the reduction of the wear area, the exposed area of the substrate of S2 decreases. Moreover, the friction area overlaps plenty of adhesion (Fig. 7b). In contrast, the wear area of S3 with the surface residual stress of -500 MPa is further reduced, with a small amount of coating peeling and adhesion (Fig. 7c). The "bonding-shedding" cycles of S3 are the fewest. It is indicated that the wear resistance of S3 tool is the best. Compared to S3, the area of the friction of S4 is similar (Fig. 7d). However, the coating peeling of S4 is intensified. Thus, the excessive surface residual compressive stress detrimentally affects the wear resistance of the coated tool.

The wear surface contains plenty of Ti and W elements is indicated in Fig. 8. A small amount of O, Al, and Si elements are also found. For one thing, the appearance of O element may cause oxidative wear and reduce the wear resistance of coated tools. For another, O element can form the products,

such as TiO_2, SiO_2, or $Si(OH)_2$, which has the function of self-lubricate, therefore reduce friction coefficient.

The results of above experiments indicate that the main wear forms of TiAlSiN coating include flake adhesion accumulation and coating peeling. With the improvement of surface residual compressive stress, the adhesion accumulation and coating peeling are reduced, resulting in the enhancement of wear resistance. However, the excessive surface residual compressive stress will adversely affect the wear resistance of the tool.

3.2 Cutting performance

3.2.1 Chip morphology

The chip morphology of TiAlSiN-coated tools with dissimilar residual stresses when the tool flank wear reaches 0.3 ± 0.02 mm is displayed in Fig. 9. With the enhancement in residual compressive stress, the chip curling degree is reduced, as can be seen from the chip macro morphology (Fig. 9a1, b1, and c1). However, the chip curling degree is increased when the surface residual compressive stress is excessive (Fig. 9d1). During high-speed cutting process, plenty of cutting heat is created at the tool tip. The cutting temperature is different between the chip surface following from rake face and the chip surface away from rake face, which causes the chip curling. Increasing the surface residual compressive stress within a certain range can reduce the generation of cutting heat, thereby reducing the degree of chip curling.

As can be seen in the chip surfaces away from rake face (Figs. 9a2, b2, c2, and d2), the severe plastic deformation is presented. Moreover, the shear banded is arranged in the
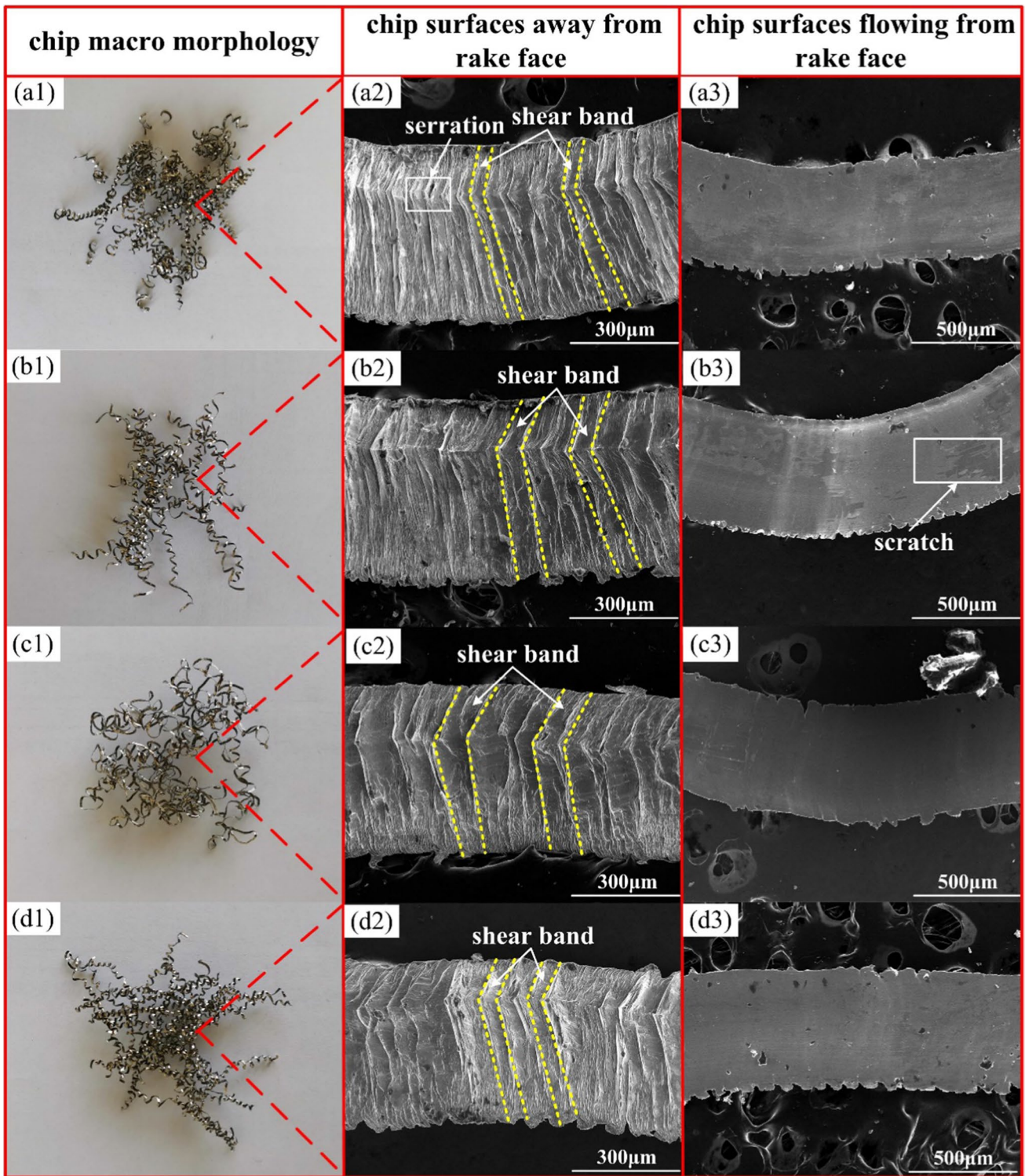
Fig. 9 Chip morphology of the coated tools with dissimilar surface residual stresses at the rapid wear stage, (a) S1, (b) S2, (c) S3, and (d) S4

direction of chip flowing. The creation of shear bands is an important feature that marks the formation of serrated chips. The serration is caused by the initiation of shear cracks and the expansion of the sliding surface, owing to

the plastic deformation of the chips at elevated temperatures [25]. In pace with the increase in surface residual compressive stress of coated tools, the chip serration spacing first increases and then decreases. This indicates

that the cutting temperature of the four coated tools first decreases and then increases. The high temperatures will reduce the stress threshold for sawtooth formation in the adiabatic shear band. The degree of thermal softening of the workpiece is more likely to be higher than the degree of strain hardening, which results in more frequent appearance of serrations.

The chip surface following from rake face is direct contact with the tool and can reflect the extent of tool wear and the machining quality [26]. The chip surface following from rake face of the coated tools S1 and S2 is rougher, which may lead to a reduction in the surface integrity of the machined surface (Figs. 9a3, b3). Compared with Figs. 9a3, b3, c3, and d3, the chip surface following from rake face becomes smoother, of which the roughness is also reduced.

It indicates that increasing the residual compressive stress on the tool surface within a certain range can effectively reduce the tool wear and improve the quality of the machined surface.

3.2.2 Cutting force

The variations of cutting force with tool wear are illustrated in Fig. 10. F_z is the main cutting force, which plays the leading role in the cutting force. It can be found that the cutting force of the TiAlSiN-coated tools has a large change in the initial and normal wear stages. It appears to increase first, then decrease and then increase. In the early stages of cutting process, the impurities and hard particles exist on the surface of both the tool and the workpiece, which enhance the
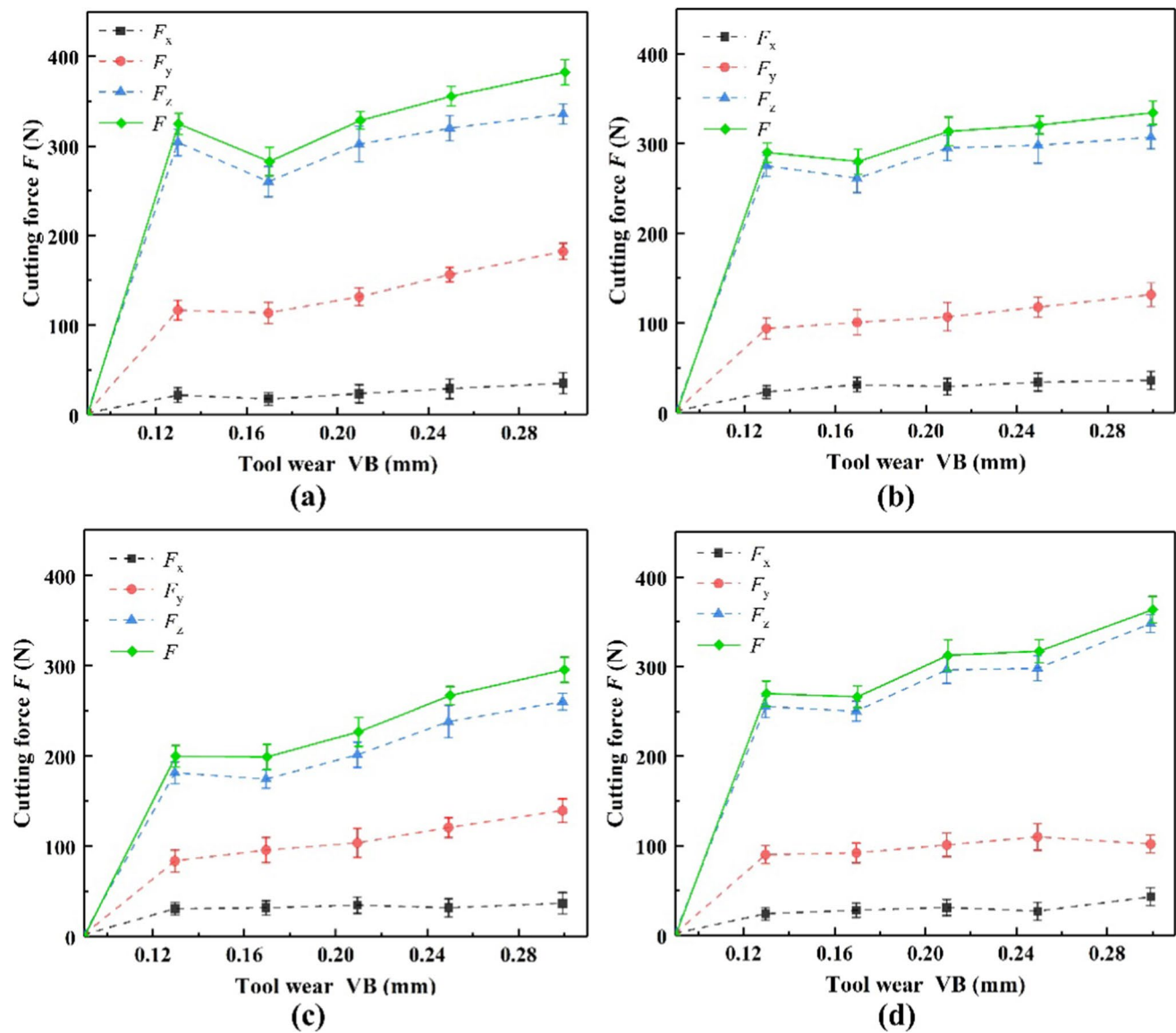

Fig. 10 Variations of cutting force with tool wear. **a** S1, **b** S2, **c** S3, and **d** S4

friction. As cutting process proceeds, the hard particles are continuously removed. The rough surface of the workpiece disappears and the friction force is reduced. So, the cutting force appears to decrease. During the rapid wear stage, the surface coating is continuously removed, resulting in the impairing of the high temperature resistance of the coating and the quick accumulation of cutting heat. Additionally, the adhesion or built-up edge is presented on the surface of the tools, which can aggravate the frictional force and the flank wear of coated tools.

During the initial and stable wear stage, coated tool S1 has the highest cutting forces among the four coated tools (Fig. 10a), which is attributed to the lowest residual surface stresses of S1. And the high cutting force can incur the low surface hardness and lower wear resistance. With the increase of surface residual compressive stress, the hardness of coated tools can be enhanced. Therefore, the cutting force of S2 is declined (Fig. 10b). The fluctuation of the cutting force is weakened, while the cutting process is more stable. When surface residual compressive stress raises up to the level of -500 MPa, the cutting force of S3 is significantly declined (Fig. 10c). The increase in surface residual compressive stress can restrain the generating and expansion of flaws, which can reduce the coating peeling. It also ensures a small friction coefficient between the tool and the chip, bringing about reduction of the cutting force. As the surface residual compressive stress further increases, the cutting force of S4 increases instead (Fig. 10d). The surface residual compressive stress will also affect the adhesion strength between the coating and the substrate. Excessive surface residual compressive stress can impair the adhesion strength and intensify the peeling of the coating, which brings about the raise of cutting force.

The cutting forces of four coated tools maintain a steady upward trend in the rapid wear stage. The surface hardness of the coated tools is enhanced at the high surface residual compressive stress, leading to the gradual reduction of

cutting forces of coated tools S1, S2 and S3 (Fig. 10a, b, and c). The magnitude of the change in cutting forces is decreased and the cutting process becomes more stable. However, the cutting force of S4 exceeds that of S2 and S3, which is close to that of S1. Excessive surface residual compressive stress can cause the brittleness of the coating, which is able to easily incur the chipping and expand the friction area between the tool flank face and the workpiece. Therefore, the cutting force of S4 increases significant.

It is concluded that the surface residual compressive stress of coated tools has a considerable effect on the cutting force. The high compressive stress can potently decrease and stabilize the cutting force, especially in the normal wear stages. However, the excessive surface residual compressive stresses can weaken the protectiveness of the coating and increase the overall cutting forces tool, which make the cutting process unstable.

3.2.3 Cutting temperature

The variations of cutting temperature with tool wear and infrared thermal image is exhibited in Fig. 11. In the initial and normal wear stage, the cutting temperatures of four coated tools rise rapidly with little difference in values. The severe work hardening of Ti6Al4V incurs high cutting force. So, a lot of cutting heat is generated. The low thermal conductivity of Ti6Al4V means that the relatively little cutting heat is dispersed out through the workpiece and the chip. The better the initial surface roughness and surface morphology of the coated tool can bring about the less friction force, which causes the less cutting heat and the lower the cutting temperature. The initial surface roughness and surface morphology of four coated tools is relatively similar (Table 3). Therefore, the cutting temperatures of the four coated tools is close during the initial and normal wear stage.

Due to the high cutting deformation and friction, the cutting temperatures of S1, S2, and S4 is sharp enhanced

Fig. 11 **a** Variations of cutting temperature with tool wear and **b** infrared thermal image
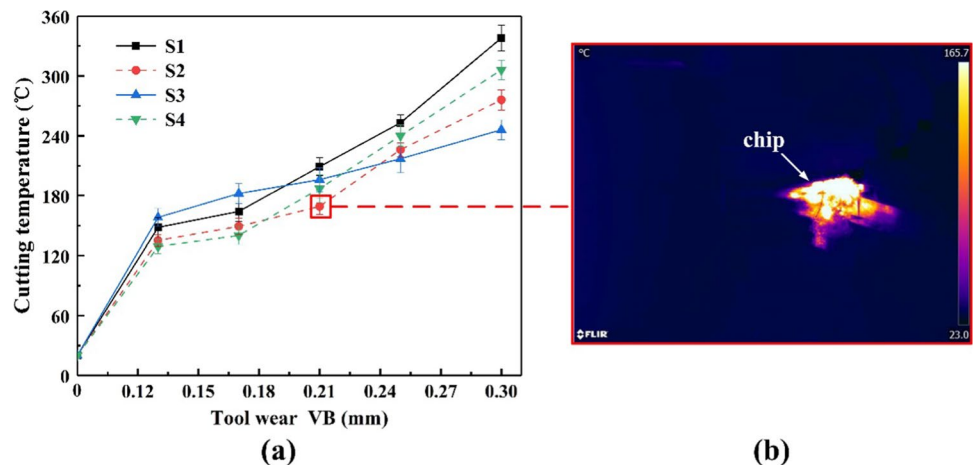
with tool wear during the rapid wear stage. However, the increase rate of cutting temperature of S3 is small. The advantage of proper compressive stress of S3 is shown in the stage of rapid wear, which can effectively reduce chip deformation and the cutting force. Therefore, in the rapid wear stage, the lowest cutting temperature of S3 is obtained.

3.2.4 Tool life

The variation of tool flank wear with cutting time is presented in Fig. 12. With the increase in residual compressive stress of the coating, the cutting life of TiAlSiN-coated tools first increases and then declines. At the surface residual compressive stress level of − 500 MPa, the maximum cutting life of the coated tool can be achieved to 26 min.

During the initial wear stage, the initial surface roughness and morphology of coated tools are the main factors affecting tool wear. According to Table 3, the surface roughness and morphology of four coated tools are similar. Therefore, the tool wear is close. As the wear intensifies, the cutting force and cutting temperature increase sharply (Figs. 10 and 11). The surface defects of the coating occur cracks under the impact of the load, which affect the coating peeling. The thermal barrier and protection of the coating is reduced, which results in the intensified tool wear and reduced tool life.

The increase of surface residual compressive stress of coating can inhibit the expansion of surface cracks and protect the coating. What is more, it can also prolong the protection time of the coating on the tool, thereby prolonging the normal wear stage of coated tools and improving the cutting life. Moreover, the surface residual compressive stress can affect the adhesion strength. When the surface residual compressive stress of coating is too large, the impact of the reduction of the adhesion strength on
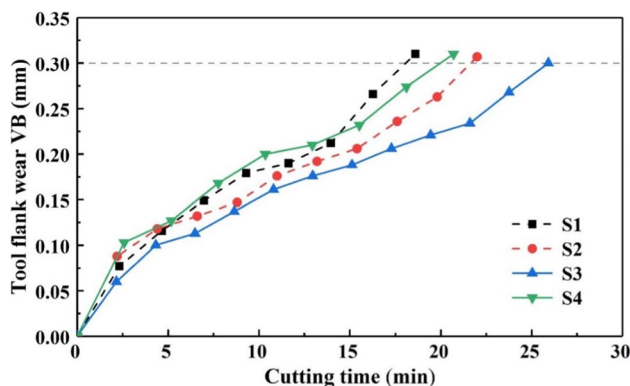

Fig. 12 Variation of tool flank wear with cutting time

the coating exceeds the suppression of crack propagation, which instead aggravates the coating peeling and incur the reducing of tool life.

3.2.5 Wear mechanism

The rake wear morphology of the TiAlSiN-coated inserts with dissimilar residual stresses is exhibited in Fig. 13. Figure 13a shows that massive crater wear can be observed, and a large-scale adhesion layer is formed by adhesion accumulating. The range of the crater is related to the high temperature and high pressure of the contact surface between the chip and the rake face. The maximum depth position is the place in which the cutting temperature is the highest. Therefore, the smaller the cutting force and the cutting temperature signifies the smaller the extent and depth of the crater wear. So, the crater wear extent of S2 is smaller than that of S1. Moreover, the large-area adhesion layer is reduced and the built-up edge is formed (Fig. 13b).

The adhesion of S3 is reduced (Fig. 13c), and the crater boundary shrinks and gradually becomes blurred. The further increase of residual compressive stress improves the micro-hardness and the wear resistance of coated tools. Thereby, the wear degree of the insert is weakened. As a result, the cutting performance of S3 is the best. The adhesion accumulation at the cutting edge of S4 is further reduced (Fig. 13d). However, the depth of the crater is significantly increased. The coating peeling is obvious, and part of the cemented carbide substrate is exposed. For one thing, the high cutting force and cutting temperature of S4 are obtained during the rapid wear stage (Figs. 10d and 11), which leads to the deeper crater wear. For another, the excessive surface residual compressive stress of the coating can decrease the adhesion strength, which aggravates the coating peeling and causes the serious rake wear.

The flank wear morphology of the TiAlSiN coated tools with dissimilar surface residual stresses is displayed in Fig. 14. Because of the low modulus of elasticity of Ti6Al4V, the workpiece rebounds greatly during cutting. The cutting state is unstable and the cutting edge of S1 appears micro-chipping (Fig. 14a). Because of the low thermal conductivity and high cutting temperature of Ti6Al4V, the coated tool is prone to bonding with the Ti6Al4V, resulting in a large area of adhesion on flank face. The scoring effect on the tool surface by hard points and the hardened layer on the machined surface causes scratches of varying depths on the flank face (Fig. 14a). Contrasted to the wear morphology of S1, the chipping phenomenon of S2 diminishes and the number of scratches decreases. Moreover, a large-scale adhesion accumulation occurs on flank face of S2 and the width of flank wear band is decreased (Fig. 14b).

The cutting edge of S3 is relatively intact and the chipping phenomenon almost disappears (Fig. 14c). In

Fig. 13 Rake wear morphology of the TiAlSiN-coated tools with dissimilar surface residual stresses: **a** S1, **b** S2, **c** S3, and **d** S4


(a)

(b)

(c)

(d)
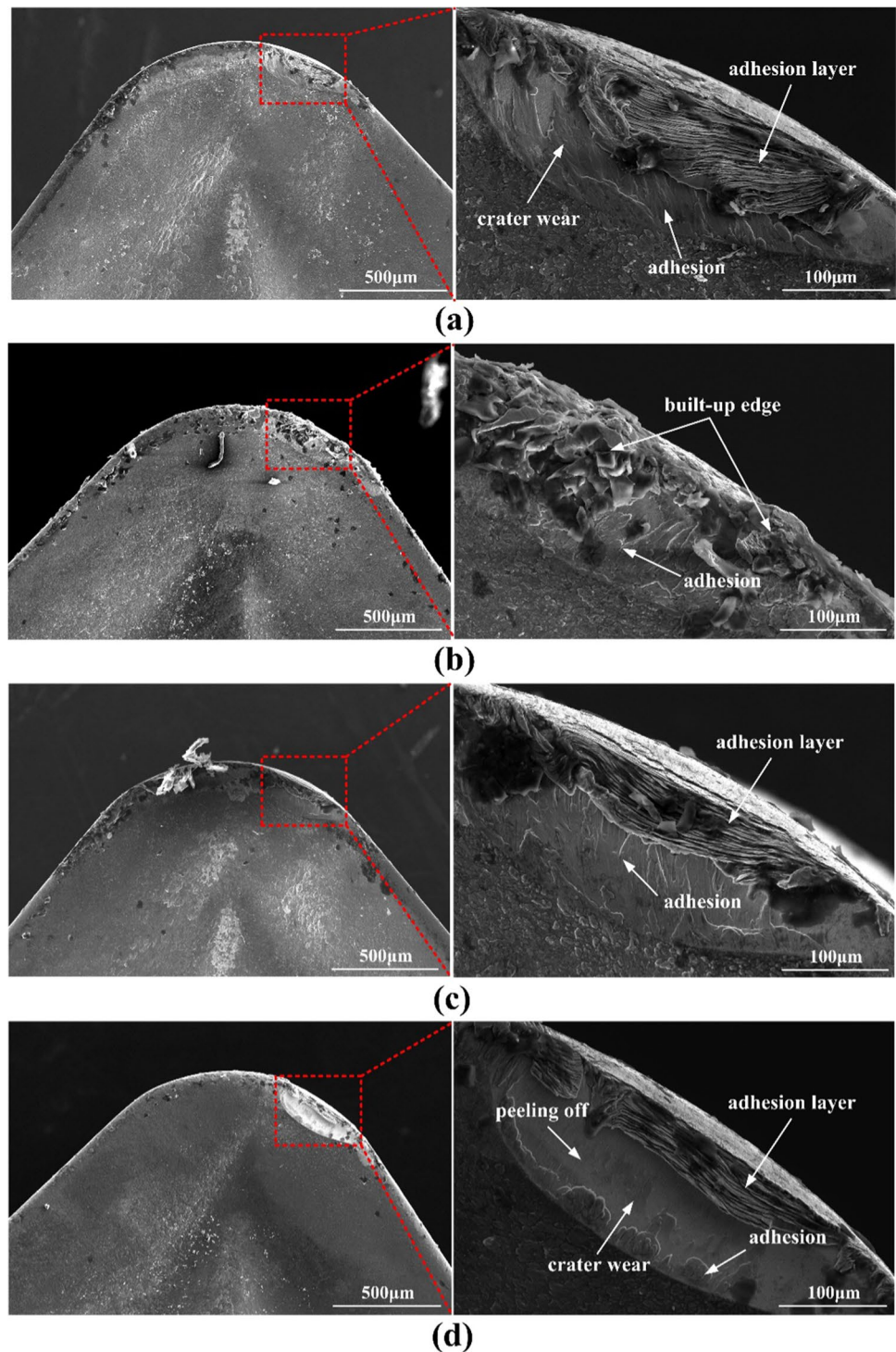
addition, the adhesion accumulation and coating peeling are significantly reduced. The wear area on the flank face is uniform. This demonstrates that the cutting process is stable without large cutting vibration at surface residual stress of -500 MPa. For the coated tool S4, the significant chipping is observed (Fig. 14d). The number of scratches and the exposed area of the cemented carbide substrate is also obviously improved. The flank face is severely worn, which indicates that excessive surface residual compressive stress can aggravate the occurrence of chipping and coating peeling.

By contrasting the wear morphology of S1-S4, the main wear forms of rake face of TiAlSiN coated tools are craters, adhesion, and adhesion layer. The main

Fig. 14 Flank wear morphology of the TiAlSiN-coated tools with dissimilar surface residual stresses. **a** S1, **b** S2, **c** S3, and **d** S4
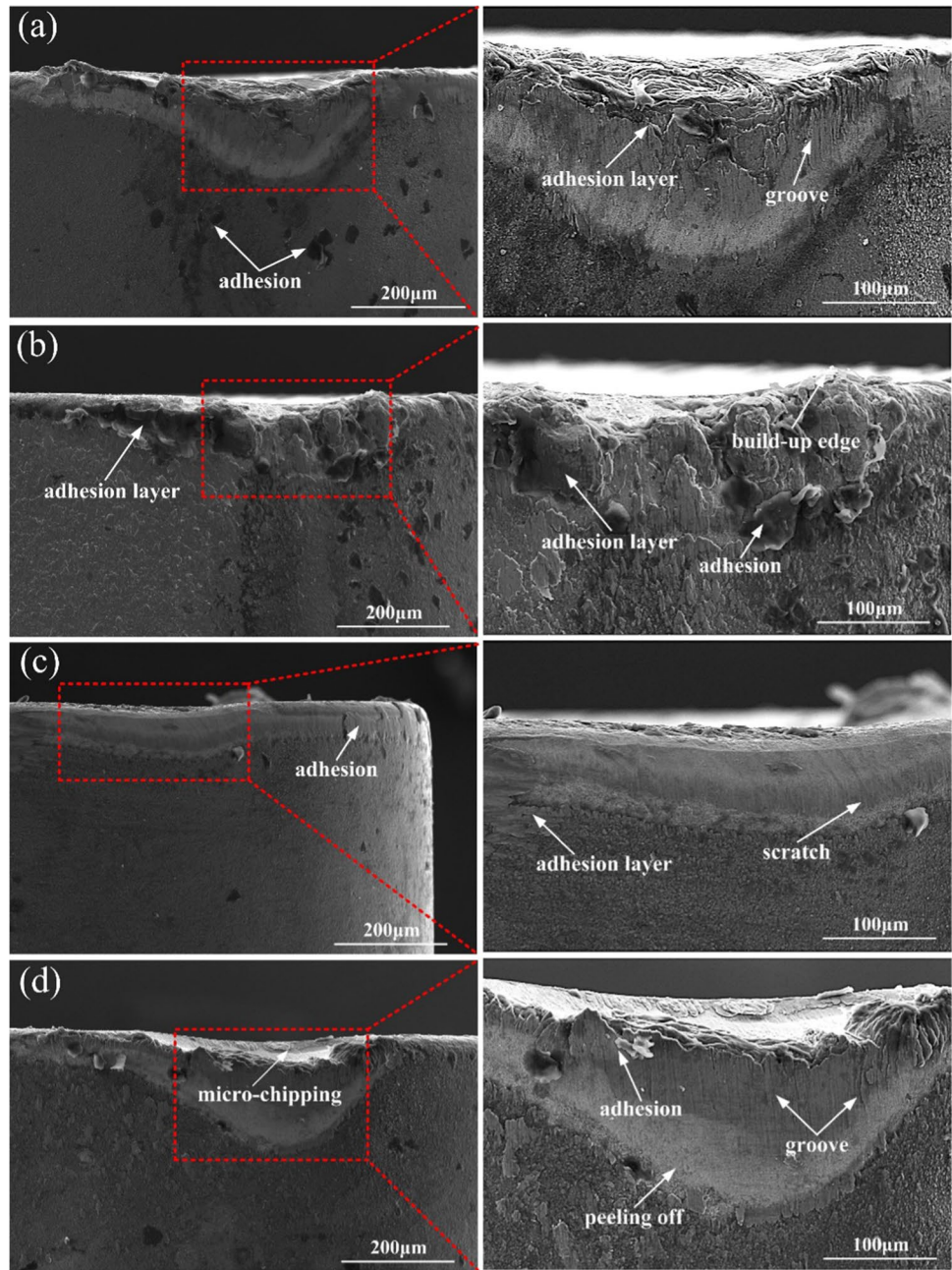
wear forms of flank face are micro-chipping, adhesion, scratches, and coating peeling. In the wake of the increase of surface residual compressive stress, the adhesion accumulation, crater wear and micro-chipping is reduced. However, the excessive surface residual compressive stress (> -500 MPa) can result in the severe micro-chipping, expand the range of abrasive wear and coating peeling. The capability of cutting of the coated insert will be deteriorated.

4 Conclusions

(1) During high-speed sliding wear process, an appropriate surface residual compressive stress can effectually decrease the friction coefficient and wear rate, which can enhance the wear resistance of the TiAlSiN coating.

(2) An appropriate residual compressive stress in the coating layer can reduce the cutting temperature and prevent chip curling. And then, the chip adhesion is

reduced in high-speed dry turning of Ti6Al4V. It also significantly reduces the cutting forces and improves process stability. However, an excessively high compressive stress leads to an increase in cutting temperatures and cutting forces.

(3) The main wear form of TiAlSiN coating is coating layer peeling and adhesion in the sliding wear process. In contrast, crater wear, adhesion accumulation, coating peeling, and micro-chipping occurred in the high-speed turning process. An appropriate surface residual compressive stress can reduce adhesion accumulation and micro-chipping.

(4) For PVD-TiAlSiN coated tools, the highest wear resistance can be obtained at a surface residual compressive stress of around -500 MPa.

The wear resistance of coated tools can be improved by optimizing the coating surface treatment process. There observation will facilitate further investigation on the more types of coated tools and surface treatment process.

Declarations

References

1. Kumar TS, Prabu SB, Manivasagam G, Padmanabhan KA (2014) Comparison of TiAlN, AlCrN, and AlCrN/TiAlN coatings for cutting-tool applications. Int J Miner Metall Mater 21(08):796–805. https://doi.org/10.1007/s12613-014-0973-y

2. Li AH, Zhao J, Zang J, Zheng W (2016) Design and simulation of thermal residual stresses of coatings on wc-co cemented carbide cutting tool substrate. J Mech Sci Technol 30(8):3777–3783. https://doi.org/10.1007/s12206-016-0430-0

3. Zhao JF, Liu ZQ, Wang B, Hu JR, Wan Y (2021) Tool coating effects on cutting temperature during metal cutting processes: comprehensive review and future research directions. Mech Syst Signal Process 150(7–8):107302. https://doi.org/10.1016/j.ymssp.2020.107302

4. Chowdhury MSI, Bose B, Yamamoto K, Shuster LS, Paiva J, Fox-Rabinovich GS, Veldhuis SC (2020) Wear performance investigation of PVD coated and uncoated carbide tools during high-speed machining of TiAl6V4 aerospace alloy. Wear 446–447:203168. https://doi.org/10.1016/j.wear.2019.203168

5. Cui XB, Guo YH, Guo JX, Ming PM (2020) Bio-inspired design of cleaner interrupted turning and its effects on specific cutting energy and harmful gas emission. J Clean Prod 271:122354. https://doi.org/10.1016/j.jclepro.2020.122354

6. Cui XB, Sun NN, Guo JX, Ma JJ, Ming PM (2022) Green multi-biomimetic spontaneous oil-transport microstructure and its effects on energy consumption in sustainable intermittent cutting. J Clean Prod 367:133035. https://doi.org/10.1016/j.jclepro.2022.133035

7. Cui XB, Duan SQ, Guo JX, Ming PM (2022) Bionic multifunctional surface microstructure for efficient improvement of tool performance in green interrupted hard cutting. J Mater Process Technol 305:117587. https://doi.org/10.1016/j.jmatprotec.2022.117587

8. Hou M, Mou W, Yan G, Song G, Wu Y, Ji W, Jiang Z, Wang W, Qian C, Cai Z (2020) Effects of different distribution of residual stresses in the depth direction on cutting performance of TiAlN coated WC-10wt%Co tools in milling Ti-6Al-4V. Surf Coat Technol 397:125972. https://doi.org/10.1016/j.surfcoat.2020.125972

9. Chaus AS, Sitkevich MV, Pokorný P, Sahul M, Haršáni M, Babincová P (2021) Wear resistance and cutting performance of high-speed steel ball nose end mills related to the initial state of tool surface. Wear 472–473:203711. https://doi.org/10.1016/j.wear.2021.203711

10. Breidenstein B, Denkena B, Vetter J, Richter B (2016) Influence of the residual stress state of coatings on the wear behavior in external turning of AISI 4140 and Ti–6Al–4V. Prod Eng Res Devel 10(2):147–155. https://doi.org/10.1007/s11740-015-0650-7

11. Bobzin K, Brögelmann T, Maier HJ, Heidenblut T, Kahra C, Carlet M (2021) Influence of residual stresses in hard tool coatings on the cutting performance. J Manuf Process 69:340–350. https://doi.org/10.1016/j.jmapro.2021.08.011

12. Gonzalo O, Navas VG, Coto B, Bengoetxea I, Gopegi UR, Etxaniz M (2011) Influence of the coating residual stresses on the tool wear. Procedia Eng 19(1):106–111. https://doi.org/10.1016/j.proeng.2011.11.087

13. Tillmann W, Grisales D, Stangier D, Thomann CA, Debus J, Nienhaus A, Apel D (2020) Residual stresses and tribomechanical behaviour of TiAlN and TiAlCN monolayer and multilayer coatings by DCMS and HiPIMS. Surf Coat Technol 406:126664. https://doi.org/10.1016/j.surfcoat.2020.126664

14. Maiti AK, Mukhopadhyay N, Raman R (2009) Improving the wear behavior of WC-CoCr-based HVOF coating by surface grinding. J Mater Eng Perform 18:1060. https://doi.org/10.1007/s11665-009-9354-5

15. Oladijo OP, Luzin V, Maledi NB, Setswalo K, Ntsoane TP, Abe H (2020) Residual stress and wear resistance of HVOF Inconel 625 coating on SS304 steel substrate. J Therm Spray Technol 29(1):1382–1395. https://doi.org/10.1007/s11666-020-01066-x

16. Özkan D, Alper YM, Szala M, Türküz C, Chocyk D, Tunç C, Göz O, Walczak M, Pasierbiewicz K, Barış YM (2021) Effects of ceramic-based CrN, TiN, and AlCrN interlayers on wear and friction behaviors of AlTiSiN+TiSiN PVD coatings. Ceram Int 47(14):20077–20089. https://doi.org/10.1016/j.ceramint.2021.04.015

17. Breidenstein B, Denkena B (2013) Significance of residual stress in PVD-coated carbide cutting tools. CIRP Ann Manuf Technol 62(1):67–70. https://doi.org/10.1016/j.cirp.2013.03.101

18. Yang J, Odén M, Johansson-Jõesaar MP, Llanes L (2014) Grinding effects on surface integrity and mechanical strength of WC-Co cemented carbides. Procedia CIRP 13(1):257–263. https://doi.org/10.1016/j.procir.2014.04.044

19. Denkena B, Breidenstein B, Wagner L, Wollmann M, Mhaede M (2013) Influence of shot peening and laser ablation on residual stress state and phase composition of cemented carbide cutting inserts. Int J Refract Met Hard Mater 36:85–89. https://doi.org/10.1016/j.ijrmhm.2012.07.005

20. Nikola K, Eric B, Patrice P, Cyril G, Christoph K, Christian L, Jamasp J, Roland E, Logé, (2017) 3D laser shock peening — a new method for the 3D control of residual stresses in selective laser melting. Mater Des 130:350–356. https://doi.org/10.1016/j.matdes.2017.05.083

21. Skordaris G, Bouzakis KD, Kotsanis T, Charalampous P, Bouzakis E, Breidenstein B, Bergmann B, Denkena B (2017) Effect of PVD film's residual stresses on their mechanical properties, brittleness, adhesion, and cutting performance of coated tools. CIRP J Manuf Sci Technol 18:145–151. https://doi.org/10.1016/j.cirpj.2016.11.003

22. Liu CY, Liu ZQ, Wang B (2018) Modification of surface morphology to enhance tribological properties for CVD coated cutting tools through wet micro-blasting post-process. Ceram Int 44:3430–3439. https://doi.org/10.1016/j.ceramint.2017.11.142

23. Tanaka S, Shirochi T, Nishizawa H, Metoki K, Miura H, Hara H, Takahashi T (2016) Micro-blasting effect on fracture resistance of PVD-AlTiN coated cemented carbide cutting tools. Surf Coat Technol 308:337–340. https://doi.org/10.1016/j.surfcoat.2016.07.094

24. Chang K, Zheng G, Cheng X, Xu R, Li Y, Yu Z, Yang X (2021) Surface integrity evolution and wear evolution of the micro-blasted coated tool in high-speed turning of Ti6Al4V. The Int J Adv Manuf Technol 115:603–616. https://doi.org/10.1007/s00170-021-07227-8

25. Behera GC, Thrinadh J, Datta S (2021) Influence of cutting insert (uncoated and coated carbide) on cutting force, tool-tip temperature, and chip morphology during dry machining of Inconel 825. Mater Today: Proceed 38(5):2664–2670. https://doi.org/10.1016/j.matpr.2020.08.332

26. Wang QQ, Jin ZJ, Zhao Y, Niu L, Guo J (2021) A comparative study on tool life and wear of uncoated and coated cutting tools in turning of tungsten heavy alloys. Wear 482–483:203929. https://doi.org/10.1016/j.wear.2021.203929